Deterministic generation of bright polarization squeezed state of light resonant with the rubidium D1 absorption line

LIANG WU,[1] YANHONG LIU,[1] RUIJIE DENG,[1] ZHIHUI YAN,[1,2,*] XIAOJUN JIA,[1,2] AND KUNCHI PENG[1,2]

[1]*State Key Laboratory of Quantum Optics and Quantum Optics Devices, Institute of Opto-Electronics, Shanxi University, Taiyuan 030006, China*
[2]*Collaborative Innovation Center of Extreme Optics, Shanxi University, Taiyuan 030006, China*
Corresponding author: zhyan@sxu.edu.cn

A polarization squeezed optical beam can directly interact with the atomic medium, and its measurement is local-oscillator free. Here we have deterministically generated polarization squeezed light at 795 nm. First, a laser at 398 nm is produced from second-harmonic generation with an enhancement cavity. Then a pair of quadrature amplitude squeezed optical fields is prepared with two degenerate optical parameter amplifiers that are pumped by the resulting laser at 398 nm. Finally, the polarization squeezed state of light is generated by combining the above two quadrature amplitude squeezed optical beams on a polarizing beam splitter, and the quantum fluctuations of three Stokes operators simultaneously are reduced 4.0 dB below the quantum noise limit. The polarization squeezing has potential applications in future quantum information networks.   © 2016 Optical Society of America

1. INTRODUCTION

Squeezing is the central concept of quantum mechanics, and the building block for application of quantum information and quantum measurement [1,2]. In both discrete-variable (DV) and continuous-variable (CV) quantum information, squeezed light and single photons are the important resources for constructing quantum entanglement [3,4], and have been applied in various kinds of quantum information protocols, such as quantum teleportation, quantum computation, quantum secret sharing, and so on [5–10]. Meanwhile, quantum information networks involving both light and matter are the key step toward practical applications of quantum information, where light can be utilized for transmitting the quantum information, and matter is able to be used as a quantum node to store and process quantum information [11]. Atoms are one of the suitable candidates of quantum nodes due to good atomic coherence [12–18]. In the past decade, the atom-based quantum memory of the nonclassical state of optical fields has been experimentally demonstrated [19–21]. The rubidium atom is a well-understood medium, and quadrature squeezed state of light resonant with the rubidium atomic absorption line has been experimentally generated by means of optical parametric downconversion [22–24].

In 2002, Korolkova *et al.* proposed the concept of CV polarization squeezed state of light. The atomic spin state is described by Stokes operators on a Bloch sphere, and comparatively the polarization of light is represented by the Stokes operators on a Poincaré sphere [25]. The polarization of light can directly interact with the spin wave of an atomic ensemble, which can be used as a quantum interface between atoms and light, and its measurement is independent of a local oscillator. As such, the polarization of light is a key resource for long-distance quantum communication or quantum memory [21,26]. In balanced homodyne detection, the phase fluctuation of interference locking of signal and local oscillator is large after the signal passes the long-distance fiber or memory medium. Fortunately, the local oscillator-free measurement of polarization squeezed light can overcome this problem. Additionally, atomic spin squeezing for quantum metrology can be obtained by mapping squeezing from light into atoms [2]. For long-distance quantum communication, the polarization squeezing at the optical fiber transmission window was generated by G. Leuchs's group with an asymmetric fiber-optic Sagnac interferometer and applied in the distribution of polarization squeezed states through an atmospheric channel [26]. A quantum node needs the polarization squeezing resonant with an atomic absorption line, and polarization squeezing at

852 nm was also produced by E. Giacobino's group based on a cloud of cold cesium atoms in a high-finesse optical cavity [27]. An alternative approach for generating polarization squeezing is based on the degenerate optical parametric amplifiers (DOPAs) below the threshold and polarizing beam splitter (PBS). The polarization squeezed state of light at 1064 nm is produced by combining two quadrature squeezed states on a PBS [28]. The tripartite polarization entangled states of bright optical beams have been theoretically investigated and experimentally generated by transforming the quadrature entanglement into polarization entanglement [29,30]. Polarization squeezing at the rubidium absorption line is demanded in the quantum Internet, because the polarization of light can directly interact with atomic spin. Additionally, the measurement of polarization of light does not need a local oscillator, and it has advantages in the quantum memory. The purpose of this experiment is to produce polarization squeezing at the rubidium absorption line by employing the optical parametric amplifier (OPA) and PBS. The polarization squeezing resonant with the rubidium absorption line is also required for constructing different kinds of quantum-entangled states of optical fields, and thus polarization squeezing is the building block for quantum information networks.

In this paper, we have deterministically generated a CV polarization squeezed state of light resonant with the rubidium D1 absorption line. We first realize the cavity-enhanced second-harmonic generation (SHG) of 795 nm laser when the influence of the thermal effect caused by PPKTP's (periodically poled potassium titanyl phosphate) absorption at short wavelength is taken into account. Then a pair of quadrature amplitude squeezed states of light is generated based on two DOPAs. Finally, the polarization squeezed state of light is obtained by combining the two quadrature squeezed beams on a PBS, and quantum noises of three Stokes operators are all −4.0 dB. The resulting polarization squeezing source is a fundamental resource for a quantum interface between light and atom. There are three key features of the polarization squeezing source in our work. First, the polarization squeezed optical fields can directly associate with the atomic ensemble. Second, the wavelength of the polarization squeezed optical fields can be easily tuned to realize the resonance with the rubidium atom, due to the Ti:sapphire laser's well-known tunable advance. Third, the local oscillator-free measurement of polarization squeezing can overcome the problem of the phase-locking fluctuation of balanced homodyne detection in quantum communication and quantum memory.

In the following, we will briefly describe the schematic of generation of CV polarization squeezed state in Section 2. First, the cavity-enhanced SHG of 795 nm is theoretically analyzed and experimentally obtained in Section 2.A. In the following, a pair of 795 nm quadrature squeezing is generated based on two DOPAs in Section 2.B. In Section 2.C, the quadrature squeezing is transformed into the polarization squeezing. Finally, we will give a brief conclusion in Section 3.

2. SCHEMATIC OF GENERATING BRIGHT POLARIZATION SQUEEZED LIGHT FOR A RUBIDIUM ATOM

In the quantum world, vacuum is not absolutely quiet, and its noise is considered as quantum noise limit (QNL). However, a
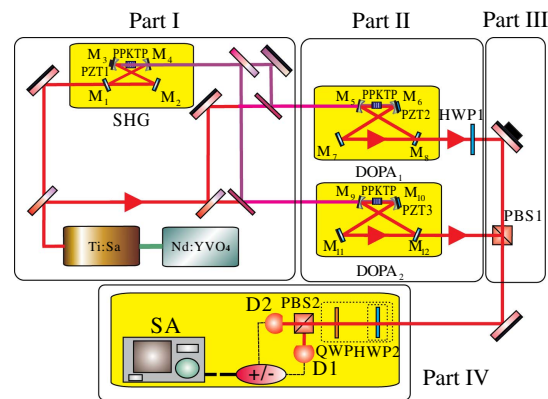

Fig. 1. Schematic of generation system of polarization squeezing. Nd:YVO4, Nd:YVO4 green laser; Ti:Sa, titanium sapphire laser; M1-12, mirrors; PZT1-3, piezoelectric transducers; PBS1-2, polarizing beam splitters; HWP1-2, half-wave plates; QWP, quarter-wave plate; ±, power positive/negative combinators; D1-2, photodetectors; SA, spectrum analyzer.

squeezed state can reduce quantum noise of one physical quantity below QNL, while that of the other conjugate physical quantity is increased above QNL to satisfy the Heisenberg uncertainty relation. The polarization squeezed state of light resonant with a rubidium D1 absorption line is unconditionally generated by combining a pair of quadrature squeezed optical fields from two DOPAs on a PBS; the generation system, including four parts, is shown in Fig. 1. The first part is the light source to produce the seed fields and pump fields for DOPAs. The Ti:sapphire laser is suitable for the interaction of light and atom as a result of its good frequency-tunable character and low noise. An external cavity-enhanced frequency doubler from 795 nm to 398 nm is first realized, and the resulting 398 nm laser is used as the pump fields of DOPAs together with the Ti:sapphire laser as the seed fields of the DOPAs. The second part, composed of two sets of DOPAs, is employed to generate a pair of quadrature amplitude squeezed optical fields. The third part is the transformation system of quadrature squeezing into polarization squeezing by combining two beams of quadrature amplitude squeezed beams with the same power and zero phase difference on a PBS. The fourth part is the measurement system of Stokes operators of light.

A. Production of Laser at 398 nm Based on SHG with Enhancement Cavity

The laser at 398 nm is usually generated by a cavity-enhanced frequency doubler of near-infrared laser. The quasi-phase-matched nonlinear crystal PPKTP has the advantage of high nonlinear coefficient and no walk-off effect. However, the SHG process is limited by the absorption of PPKTP at short wavelength and associated thermal effect, and cavity-enhanced SHG employs a bow tie-type ring configuration instead of the standing wave cavity in order to reduce the influence of the thermal effect of the PPKTP crystal [31].

We start by studying the dependence of the second-harmonic wave output power P_2 through SHG cavity on the fundamental wave input power P_1, which can be written as [32]

$$\sqrt{\frac{P_2}{P_1}}\left[2-\sqrt{1-T}\left(2-L-\Gamma\sqrt{\frac{P_2}{E_{NL}}}\right)\right]^2 - 4T\sqrt{E_{NL}P_1} = 0,$$

(1)

where T is the transmission coefficient of the input coupler for the fundamental wave, and L is the total linear losses in the cavity exclusive of T for the fundamental wave. Γ ($\Gamma = E_{NL} + \Gamma_{abs}$) is the nonlinear depletion. The single-pass nonlinear conversion efficiency E_{NL} of the PPKTP is measured to be 1.28%/W with the same focusing condition in the actual resonant cavity, and Γ_{abs} ($\Gamma_{abs} = P_{abs}/P_C^2$) is the absorption efficiency of the SHG process, where P_{abs} and P_C are the absorbed and circulating power in the SHG cavity.

Thus the optimized transmissivity of the input coupler for the fundamental wave T^{opt} can be obtained as

$$T^{opt} = \frac{L}{2} + \sqrt{\left(\frac{L}{2}\right)^2 + \Gamma P_1}.$$

(2)

When the fundamental wave power P_1 is 1 W, the optimal transmissivity of the input coupler for the fundamental wave should be $T^{opt} \simeq 13\%$, which corresponds to an impedance-matched cavity.

The light source part, composed of the Ti:sapphire laser and the external cavity-enhanced frequency doubler, is illustrated in part I of Fig. 1. The Ti:sapphire laser and SHG laser are used as the seed fields and the pump fields for DOPA, respectively. The Ti:sapphire laser (Coherent Inc. MBR110) pumped by 15 W power of Nd:YVO4 green laser (Yuguang DPSS FG-VIIIB) outputs 2.7 W laser at 795 nm. The external cavity enhanced SHG has a four-mirror ring cavity configuration, consisting of two flat mirrors (M1, M2), two spherical mirrors (M3, M4) with 100 mm radius of curvature, and a 1 mm × 2 mm × 10 mm type-I phase-matching PPKTP crystal. The flat mirror M1, with transmissivity of 13% at 795 nm, is used as the input coupler of the SHG cavity, and the spherical mirror M4 with high-reflection at 795 nm and antireflection at 398 nm is used as the output coupler of the SHG cavity. The other two mirrors (M2, 3) are high-reflection at 795 nm. The piezo-electric transducer (PZT) mounted on M3 is used to realize the input fundamental wave resonance in the cavity by the Pound–Drever–Hall (PDH) technique.

In our experiment, 380 mW SHG light is produced when the mode-matched input fundamental wave light power is 1 W. As the fundamental wave power is reduced to 627 mW, stable 279 mW SHG light is obtained, with the maximum conversion efficiency $\eta = 44.5\%$.

The dependence of the second-harmonic wave output power on the incident fundamental wave input power is shown in Fig. 2. Trace (i) [(ii)] is the theoretical output curve of SHG without (with) crystal's absorption at 398 nm, and trace (iii) is the measured SHG cavity output power [32]. We find that our experimental data can be fitted with the theoretical value when the injected fundamental wave power is less than 650 mW, but after that point, a gap appears between the experimental result and theoretical value due to the poor locking caused by the bistable effect.
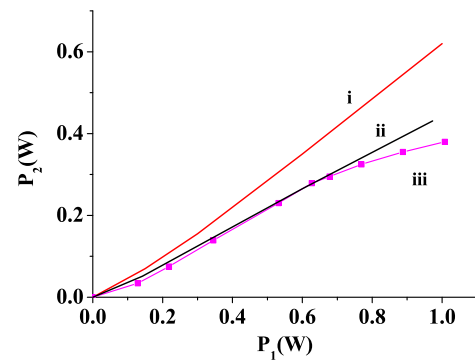

Fig. 2. Dependence of the second-harmonic wave output power on the fundamental wave input power.

B. Generating a Pair of Bright Quadrature Amplitude Squeezed States by Utilizing DOPAs

In quantum optics, light is described by annihilation operator $\hat{a}$, and its real and imaginary parts correspond to the amplitude quadrature $\hat{X}$ and phase quadrature $\hat{Y}$. The optical parametric downconversion process is one of the efficient ways to generate quadrature squeezed states of light. The experimental setup for generation of bright quadrature squeezed light is depicted in part II of Fig. 1. DOPA1 and DOPA2 with the four-mirror ring cavity configuration consist of two spherical mirrors (M5 and M6 for DOPA1, M9 and M10 for DOPA2) with 100 mm radius of curvature, two flat mirrors (M7 and M8 for DOPA1, M11 and M12 for DOPA2) and $1 * 2 * 10$ mm^3 type-I phase-matching PPKTP crystals. The spherical mirrors (M5 and M9) are used as the input couplers of the DOPA1 and DOPA2, which are coated with antireflection at 398 nm and high-reflection at 795 nm. The flat mirrors (M8 and M12) coated with $T = 5.0\%$ for 795 nm are used as the output couplers. All the other mirrors are coated with high-reflection at 795 nm. The spherical mirrors M6 and M10 are mounted on PZTs to lock the cavity length on resonance with injected seed signals by the PDH technique. The squeezing can be maintained for several minutes with the help of the locking technique and reducing the thermal effect influence of SHG. Both DOPAs operate in the parametric deamplification as the relative phase between the pump fields and seed fields was locked to π. The beam waists of the subharmonic optical fields for DOPA1 and DOPA2 are 39 μm. The finesses of DOPA1 and DOPA2 for the subharmonic mode are 111 and 110, respectively. When the PPKTP crystal is temperature-controlled around 54.3°C, the threshold powers are 90 mW and 91 mW. Two downconverted optical fields of 0.5 mW are obtained with the pump beam powers of 40 mW and the seed beam powers of 15 mW. The coupling efficiency of two quadrature squeezed optical beams is 98.6%.

In balanced homodyne detection, the measurements of amplitude and phase quadratures of optical fields are very sensitive to the phase difference between local oscillator and signal optical fields, and the amplitude and phase quadratures can be measured by changing the interfered phase difference. Figure 3 illustrates both the squeezing and antisqueezing quantum noises of amplitude and phase quadratures measured by a
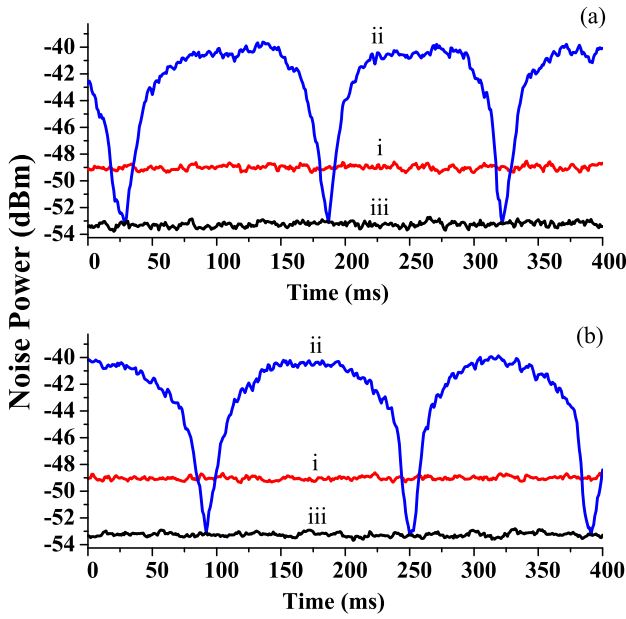
Fig. 3. Quantum fluctuations of quadrature of bright quadrature amplitude squeezed optical beams. (a) DOPA I; (b) DOPA II.

spectrum analyzer with RBW: 300 kHz, VBW: 300 Hz. Trace (i) is the QNL, trace (ii) is the quantum noise power of quadratures with phase scanning, and trace (iii) is the quantum noise power of quadratures with zero phase difference. The electronics noise level of a photodetector in balanced homodyne detection is about -77.0 ± 0.2 dBm, which is low enough for the squeezing measurement. The quantum noises of quadrature amplitude and quadrature phase of -53.0 ± 0.4 dBm and -40.0 ± 0.4 dBm are directly measured by a spectrum analyzer, and the corresponding QNL of -49.0 ± 0.2 dBm can be measured by blocking the input signal field in balanced homodyne detection. Therefore, the actual squeezing degree of quadrature amplitude is 4.0 dB at the analysis frequency of 3.0 MHz, as shown in Figs. 3(a) and 3(b), respectively.

C. Transformation of Quadrature Squeezed Optical Fields into Polarization Squeezed State

The polarization state of light is usually described by Stokes operators ($\hat{S}_0$, $\hat{S}_1$, $\hat{S}_2$, and $\hat{S}_3$) on a Poincaré sphere [25]. $\hat{S}_0$ corresponds to the intensity of optical fields and $\hat{S}_1$, $\hat{S}_2$, and $\hat{S}_3$ stand for the horizontal, diagonal, and right circular polarizations, respectively. Stokes operators are described by the annihilation operator $\hat{a}_{H(V)}$ and creation operator $\hat{a}_{H(V)}^+$ for the horizontal (vertical) polarization modes, and they are

$$
\begin{aligned}
\hat{S}_0 &= \hat{a}_H^\dagger \hat{a}_H + \hat{a}_V^\dagger \hat{a}_V, \\
\hat{S}_1 &= \hat{a}_H^\dagger \hat{a}_H - \hat{a}_V^\dagger \hat{a}_V, \\
\hat{S}_2 &= \hat{a}_H^\dagger \hat{a}_V e^{i\theta} + \hat{a}_V^\dagger \hat{a}_H e^{-i\theta}, \\
\hat{S}_3 &= (\hat{a}_H^\dagger \hat{a}_V e^{i\theta} - \hat{a}_V^\dagger \hat{a}_H e^{-i\theta})/i,
\end{aligned}
\tag{3}
$$

where θ is the relative phase between the horizontal and vertical polarization modes. When their phase difference θ is locked at 0 ($\pi/2$), quantum noises of three Stokes operators $\hat{S}_0$, $\hat{S}_1$, and

$\hat{S}_{2(3)}$ will be squeezed by combining two quadrature amplitude squeezed light on a PBS, and the Stokes operator $\hat{S}_{3(2)}$ can be squeezed with two quadrature phase squeezed light.

In our system, the layout of the transformation system of quadrature squeezing into polarization squeezing is shown in part III of Fig 1. Two mode-matched bright quadrature amplitude squeezed optical beams with the same power ($\alpha_H = \alpha_V = \alpha$), orthogonal polarization, and zero phase difference are combined on a PBS. The fluctuations of each Stokes operator can be obtained as

$$
\begin{aligned}
V_0 &= V_1 = V_2 = \alpha^2(\Delta^2 \hat{X}_H + \Delta^2 \hat{X}_V), \\
V_3 &= \alpha^2(\Delta^2 \hat{Y}_H + \Delta^2 \hat{Y}_V).
\end{aligned}
\tag{4}
$$

$\hat{X}_{H(V)}$ and $\hat{Y}_{H(V)}$ are the quadrature amplitude and phase of the downconverted optical beams, respectively.

The generation of polarization squeezing requires two identical quadrature squeezed beams and PBS with a combination ratio of 50/50. Two seed optical beams with the same power are injected into two identical DOPAs to produce two quadrature squeezed beams, and by adjusting half-wave plates before PBS1 to realize the combination ratio of 50/50. These two quadrature squeezed optical fields are combined on the PBS to be transformed into polarization squeezing. The seed optical beams and the corresponding downconverted optical beams are also used to lock the cavity resonant with the signal optical fields, and zero phase difference of interference, respectively. The detection of all Stokes operators (polarization components) is different from balanced homodyne detection, and only a half-wave plate, quarter-wave plate, PBS, two photodiodes, and power positive/negative combinator, which are shown in part IV of Fig. 1, are needed. In particular, the strong local oscillator is not required. In the measurement of Stokes operators of a polarization squeezed optical beam, the horizontal and vertical polarization modes are separated through a PBS; their sum (difference) corresponds to $\hat{S}_0$ ($\hat{S}_1$). $\hat{S}_2$ will be measured by rotating 45 deg polarization with a half-wave plate. By inserting the quarter-wave plate before the PBS, the linear polarization becomes the circular polarization, and $\hat{S}_3$ can be measured.

The quantum noises of $\hat{S}_0$, $\hat{S}_1$, $\hat{S}_2$, and $\hat{S}_3$ are measured by the spectrum analyzer with RBW: 300 kHz, VBW: 300 Hz, and depicted in Figs. 4(a)–4(d), respectively. Trace (i) is the QNL and trace (ii) is the quantum noise of the Stokes operator. The intracavity losses caused by the thermal effect of PPKTP's absorption at short wavelength is the main limitation to the observed squeezing. The PPKTP's absorption of 398 nm laser influences not only the cavity-enhanced SHG process, but also the downconversion in OPA. Besides, the other intracavity losses of mirror coating and the fluctuation of phase locking limit the squeezed degree. In the region of lower frequencies, the extra noises in the pump laser is strong, and the quantum noise of the laser is far higher than QNL. Meanwhile, quantum entanglement quality degrades in higher-frequency ranges. Thus quantum fluctuations of three Stokes operators $\hat{S}_0$, $\hat{S}_1$, $\hat{S}_2$, and $\hat{S}_3$ are directly measured by the spectrum analyzer at the analyzing frequency of 3 MHz. The corresponding QNL, which is measured by injecting the coherent light with the same power, is -61.0 ± 0.2 dBm. The quantum noises of three Stokes operators $\hat{S}_0$, $\hat{S}_1$, $\hat{S}_2$ are about -65.0 ± 0.4 dBm,
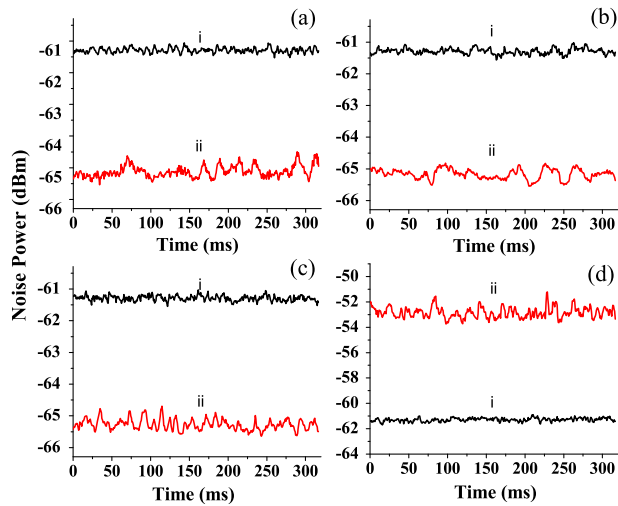
Fig. 4. Quantum noises of Stokes operators of polarization squeezed light. (a) $\hat{S}_0$; (b) $\hat{S}_1$; (c) $\hat{S}_2$; (d) $\hat{S}_3$.

which are 4.0 dB below the QNL. The corresponding quantum noise of Stokes operator $\hat{S}_3$ is -52.0 ± 0.9 dBm, that is, 9.0 dB above the QNL.

The Heisenberg uncertainty relation implies the minimum uncertainty state. According to the Heisenberg uncertainty relation, quantum fluctuations of Stokes operators ($V_j = \langle \hat{S}_j^2 \rangle - \langle \hat{S}_j \rangle^2$) satisfy the relations $V_1 V_2 \geq |\langle \hat{S}_3 \rangle|^2$, $V_2 V_3 \geq |\langle \hat{S}_1 \rangle|^2$, $V_3 V_1 \geq |\langle \hat{S}_2 \rangle|^2$. When $V_1 V_2 = |\langle \hat{S}_3 \rangle|^2$, $V_2 V_3 = |\langle \hat{S}_1 \rangle|^2$, $V_3 V_1 = |\langle \hat{S}_2 \rangle|^2$ are taken, it is the minimum uncertainty state. The minimum uncertainty state corresponds to $V_1 V_2 = V_2 V_3 = 0$, $V_3 V_1 = 4\alpha^4$. In our system, the squeezing of Stokes operators ($\hat{S}_1$, $\hat{S}_2$) is 4.0 dB, and anti-squeezing of the Stokes operator $\hat{S}_3$ is 9.0 dB; our results correspond to $V_1 V_2 = 0.61\alpha^4$, $V_2 V_3 = V_3 V_1 = 12.39\alpha^4$, as a result of finite squeezing degree limitation.

3. CONCLUSION

Quantum networks require polarization squeezing at the frequency resonant with the D1 line of rubidium atoms, because the polarization of light and the spin of atoms are described by Stokes operators, and can directly interact with each other. For the generation of CV polarization squeezed light at the frequency resonant with the rubidium absorption line, the laser at 398 nm is required to pump the DOPA. However, the influence of the thermal effect caused by the PPKTP crystal absorption at laser at 398 nm is obvious, so a ring cavity with large optical beam waist and low fundamental wave power is employed in our external cavity-enhanced SHG. Two quadrature amplitude squeezed beams are produced by two DOPAs, and then combined on a PBS with zero phase difference to be transformed into polarization squeezing, whose quantum noises of three Stokes parameters ($\hat{S}_0$, $\hat{S}_1$, $\hat{S}_2$) are simultaneously reduced 4.0 dB below QNL. The measurement does not need a local oscillator, and thus the polarization squeezing can potentially be applied in future quantum information networks.

REFERENCES

1. S. L. Braunstein and P. van Loock, "Quantum information with continuous variables," Rev. Mod. Phys. **77**, 513–577 (2005).
2. J. Hald, J. L. Sørensen, C. Schori, and E. S. Polzik, "Spin squeezed atoms: a macroscopic entangled ensemble created by light," Phys. Rev. Lett. **83**, 1319–1322 (1999).
3. X. L. Wang, L. K. Chen, W. Li, H. L. Huang, C. Liu, C. Chen, Y. H. Luo, Z. E. Su, D. Wu, Z. D. Li, H. Lu, Y. Hu, X. Jiang, C. Z. Peng, L. Li, N. L. Liu, Y. A. Chen, C. Y. Lu, and J. W. Pan, "Experimental ten-photon entanglement," arXiv:1605.08547v1 (2016).
4. X. L. Su, Y. P. Zhao, S. H. Hao, X. J. Jia, C. D. Xie, and K. C. Peng, "Experimental preparation of eight-partite cluster state for photonic qumodes," Opt. Lett. **37**, 5178–5180 (2012).
5. D. Bouwmeester, J. W. Pan, K. Mattle, M. Eibl, H. Weinfurter, and A. Zeilinger, "Experimental quantum teleportation," Nature **390**, 575–579 (1997).
6. A. Furusawa, J. L. Sørensen, S. L. Braunstein, C. A. Fuchs, H. J. Kimble, and E. S. Polzik, "Unconditional quantum teleportation," Science **282**, 706–709 (1998).
7. X. D. Cai, D. Wu, Z. E. Su, M. C. Chen, X. L. Wang, L. Li, N. L. Liu, C. Y. Lu, and J. W. Pan, "Entanglement-based quantum machine learning," Phys. Rev. Lett. **114**, 110504 (2015).
8. X. L. Su, S. H. Hao, X. W. Deng, L. Y. Ma, M. H. Wang, X. J. Jia, C. D. Xie, and K. C. Peng, "Gate sequence for continuous variable one-way quantum computation," Nat. Commun. **4**, 2828 (2013).
9. Y. A. Chen, A. N. Zhang, Z. Zhao, X. Q. Zhou, C. Y. Lu, C. Z. Peng, T. Yang, and J. W. Pan, "Experimental quantum secret sharing and third-man quantum cryptography," Phys. Rev. Lett. **95**, 200502 (2005).
10. A. M. Lance, T. Symul, W. P. Bowen, B. C. Sanders, and P. K. Lam, "Tripartite quantum state sharing," Phys. Rev. Lett. **92**, 177903 (2004).
11. H. J. Kimble, "The quantum internet," Nature **453**, 1023–1030 (2008).
12. M. D. Eisaman, A. Andre, F. Massou, M. Fleischhauer, A. S. Zibrov, and M. D. Lukin, "Electromagnetically induced transparency with tunable single-photon pulses," Nature **438**, 837–841 (2005).
13. D. J. Saunders, J. H. D. Munns, T. F. M. Champion, C. Qiu, K. T. Kaczmarek, E. Poem, P. M. Ledingham, I. A. Walmsley, and J. Nunn, "Cavity-enhanced room-temperature broadband Raman memory," Phys. Rev. Lett. **116**, 090501 (2016).
14. A. M. Marino, R. C. Pooser, V. Boyer, and P. D. Lett, "Tunable delay of Einstein-Podolsky-Rosen entanglement," Nature **457**, 859–862 (2009).
15. Z. Z. Qin, L. M. Cao, H. L. Wang, A. M. Marino, W. P. Zhang, and J. T. Jing, "Experimental generation of multiple quantum correlated beams from hot rubidium vapor," Phys. Rev. Lett. **113**, 023602 (2014).
16. L. Li, Y. O. Dudin, and A. Kuzmich, "Entanglement between light and an optical atomic excitation," Nature **498**, 466–469 (2013).
17. V. Parigi, V. D'Ambrosio, C. Arnold, L. Marrucci, F. Sciarrino, and J. Laurat, "Storage and retrieval of vector beams of light in a multiple-degree-of-freedom quantum memory," Nat. Commun. **6**, 7706 (2015).
18. D. S. Ding, W. Zhang, Z. Y. Zhou, S. Shi, B. S. Shi, and G. C. Guo, "Raman quantum memory of photonic polarized entanglement," Nat. Photonics **9**, 332–338 (2015).
19. J. Appel, E. Figueroa, D. Korystov, M. Lobino, and A. I. Lvovsky, "Quantum memory for squeezed light," Phys. Rev. Lett. **100**, 093602 (2008).
20. K. Honda, D. Akamatsu, M. Arikawa, Y. Yokoi, K. Akiba, S. Nagatsuka, T. Tanimura, A. Furusawa, and M. Kozuma, "Storage and retrieval of a squeezed vacuum," Phys. Rev. Lett. **100**, 093601 (2008).

21. K. Jensen, W. Wasilewski, H. Krauter, T. Fernholz, B. M. Nielsen, M. Owari, M. B. Plenio, A. Serafini, M. M. Wolf, and E. S. Polzik, "Quantum memory for entangled continuous-variable states," Nat. Phys. **7**, 13–16 (2010).

22. T. Tanimura, D. Akamatsu, Y. Yokoi, A. Furusawa, and M. Kozuma, "Generation of a squeezed vacuum resonant on Rubidium D1 line with periodically-poled KTiOPO₄," Opt. Lett. **31**, 2344–2346 (2006).

23. G. Hétet, O. Glöckl, K. A. Pilypas, C. C. Harb, B. C. Buchler, H. A. Bachor, and P. K. Lam, "Squeezed light for bandwidth-limited atom optics experiments at the rubidium D1 line," J. Phys. B **40**, 221–226 (2007).

24. A. Predojević, Z. Zhai, J. M. Caballero, and M. W. Mitchell, "Rubidium resonant squeezed light from a diode-pumped optical-parametric oscillator," Phys. Rev. A **78**, 063820 (2008).

25. N. Korolkova, G. Leuchs, R. Loudon, T. C. Ralph, and C. Silberhorn, "Polarization squeezing and continuous-variable polarization entanglement," Phys. Rev. A **65**, 052306 (2002).

26. C. Peuntinger, B. Heim, C. R. Müller, C. Gabriel, C. Marquardt, and G. Leuchs, "Distribution of squeezed states through an atmospheric channel," Phys. Rev. Lett. **113**, 060502 (2014).

27. V. Josse, A. Dantan, L. Vernac, A. Bramati, M. Pinard, and E. Giacobino, "Polarization squeezing with cold atoms," Phys. Rev. Lett. **91**, 103601 (2003).

28. W. P. Bowen, R. Schnabel, H.-A. Bachor, and P. K. Lam, "Polarization squeezing of continuous variable Stokes parameters," Phys. Rev. Lett. **88**, 093601 (2002).

29. Z. H. Yan and X. J. Jia, "Direct production of three-color polarization entanglement for continuous variable," J. Opt. Soc. Am. B **32**, 2139–2145 (2015).

30. L. Wu, Z. H. Yan, Y. H. Liu, R. J. Deng, X. J. Jia, C. D. Xie, and K. C. Peng, "Experimental generation of tripartite polarization entangled states of bright optical beams," Appl. Phys. Lett. **108**, 161102 (2016).

31. W. H. Yang, Y. J. Wang, Y. H. Zheng, and H. D. Lu, "Comparative study of the frequency-doubling performance on ring and linear cavity at short wavelength region," Opt. Express **23**, 19624–19633 (2015).

32. R. Le Targat, J. J. Zondy, and P. Lemonde, "75%-efficiency blue generation from an intracavity PPKTP frequency doubler," Opt. Commun. **247**, 471–481 (2005).